



**HAL**  
open science

## Numerical and experimental approaches to characterize the mass transfer process in wood elements

Tuan Anh Nguyen, Nicolas Angellier, Sabine Caré, Laurent Ulmet, Frédéric  
Dubois

► **To cite this version:**

Tuan Anh Nguyen, Nicolas Angellier, Sabine Caré, Laurent Ulmet, Frédéric Dubois. Numerical and experimental approaches to characterize the mass transfer process in wood elements. Wood Science and Technology, 2017, 51 (4), pp.811 - 830. 10.1007/s00226-017-0898-5 . hal-01711379

**HAL Id: hal-01711379**

**<https://enpc.hal.science/hal-01711379>**

Submitted on 30 Apr 2019

**HAL** is a multi-disciplinary open access archive for the deposit and dissemination of scientific research documents, whether they are published or not. The documents may come from teaching and research institutions in France or abroad, or from public or private research centers.

L'archive ouverte pluridisciplinaire **HAL**, est destinée au dépôt et à la diffusion de documents scientifiques de niveau recherche, publiés ou non, émanant des établissements d'enseignement et de recherche français ou étrangers, des laboratoires publics ou privés.

1           **Numerical and Experimental Approaches to Characterize**  
2           **the Mass Transfer Process in Wood Elements**

3 Tuan Anh N’Guyen<sup>(1)</sup>, Nicolas Angellier<sup>(1)</sup>, Sabine Caré<sup>(2)</sup>, Laurent Ulmet<sup>(1)</sup>,  
4 Frédéric Dubois<sup>(1)</sup>

5 *<sup>(1)</sup> Heterogeneous Materials Research Group (EA 3178), University of Limoges, F-19300*  
6 *Egletons, France*

7 *<sup>(2)</sup> Laboratoire Navier, UMR8205, Ecole des Ponts, IFSTTAR, CNRS, UPE, Champs-sur-*  
8 *Marne, France*

9 Corresponding author: Nicolas Angellier, Campus Universitaire de Génie Civil,  
10 17 Boulevard Jacques Derche, 19300 Egletons

11 Phone: (+33) 555 934 520, Fax: (+33) 555 934 501, e-mail: [nicolas.angellier@unilim.fr](mailto:nicolas.angellier@unilim.fr)

12  
13 **Abstract:** The scope of this paper is an experimental characterization of diffusion  
14 parameters for wood material. Based on a nonlinear mass transfer algorithm, the present  
15 study focuses on the need to capture experimental moisture profiles in the sample, along  
16 with its evolution in weighting during both the desorption and adsorption phases,  
17 especially when the moisture content of the samples is far from the equilibrium state  
18 inducing a great gradient between heart and exchange surfaces of specimen. These  
19 moisture profiles are derived by means of a gammadensimetry laboratory method based  
20 on the water adsorption of gamma rays. The determination of the diffusion parameters  
21 obtained through optimizing a simulation by means of implementing the mass transfer  
22 kinetics into a finite difference method. Both the diffusion coefficient and convective  
23 exchange coefficient are deduced by considering a Nelder-Mead simplex inversion  
24 method. This work highlights the efficiency of the approach dedicated to uncoupling  
25 nonlinear diffusion in the cross-sections from boundary conditions in terms of convective

26 exchanges and equilibrium moisture. Scale effects and boundary conditions are also  
27 investigated herein.

28 **Keywords:** Moisture content, Wood material, Mass transfer, Gammadensimetry,  
29 Diffusion model, Inverse methods.

30

## 31 **1 - Introduction**

32 In pursuit of sustainable development goals, greater numbers of timber elements are being  
33 used in many types of public construction like buildings and bridges. The demand for  
34 timber construction today is constantly rising, yet many technological obstacles still  
35 prevent the wider use of wood in the highly competitive field of construction materials.

36 When placed in outdoor conditions or heat spaces, these elements are subjected to  
37 moisture content variations induced by a non-stabilized equilibrium between wood and  
38 the climatic environment. The moisture content gradient, associated with the orthotropy  
39 of wood, induces hydric stresses amplified by the hyperstaticity level or the coupling with  
40 other materials, such as concrete or steel in the case of composite structures. The  
41 magnitude of these stresses is not well known at the design stage and not seriously taken  
42 into account in construction regulations. This mechanical state can induce a degradation  
43 in toughness and the appearance of cracks. In order to facilitate timber structure  
44 development, the issue of moisture content needs to be addressed by the scientific  
45 community.

46 This context requires in particular developing an *in situ* monitoring protocol. The control  
47 of moisture content mapping through a cross-section is currently limited by resistive  
48 methods that rely on the use of surface electrodes, which allow for the estimation, after  
49 calibration, of moisture to a depth of around 1 cm (Dubois *et al.*, 2006). This inadequate

50 method needs to be complemented by numerical simulations in order to deduce moisture  
51 content gradients and their evolution vs. time by taking into account temperature and  
52 humidity in the climatic environment (Manfoumbi, 2012; Manfoumbi, 2014). This  
53 approach however imposes several limitations. First of all, the diffusion properties  
54 introduced into numerical simulations must be correctly estimated by determining the  
55 nonlinear diffusion coefficients. Secondly, the simulation must integrate surface  
56 exchanges by considering the convective effects in terms of temperature and humidity.  
57 As a final step, specific thermo-hygro-mechanical behavior must be considered when  
58 estimating the thermo-hygro stresses (Dubois *et al.*, 2012; Colmars *et al.*, 2014).  
59 The present work pertains to the first step and is intended to determine the diffusion  
60 parameters. The characterization protocol is typically based on the double weighing  
61 principle. For various sample geometries (at the centimeter scale), this technique consists  
62 of optimizing the diffusion parameters in accordance to their corresponding average  
63 moisture content during adsorption and desorption tests. The main difficulty lies in  
64 separating the effects of boundary conditions, including sorption hysteresis and surface  
65 humidity exchanges. Numerical algorithms, derived from a minimization step between  
66 experimental and numerical differences, do not always yield a unique realistic solution.  
67 Moreover, in the case of samples far from the equilibrium state, errors on the  
68 identifications of the diffusion properties may be done due to insufficient measurement  
69 points. In this case, the method doesn't allow the uncoupling between the diffusion to the  
70 heart and the surface exchanges between first fibers and the climatic environment.  
71 To overcome this inconsistency and to highlight how the choice of the experimental  
72 measurements may influence the identification of the diffusion parameters, the present  
73 paper provides an additional experimental test on larger samples (at the decimeter scale),  
74 thus making it possible to generate a moisture content profile measured with the

75 gammadensimetry technique. Three boundary condition tests have been taken into  
76 account in order to demonstrate the relevance of this method and its robustness. The first  
77 section will describe the experimental set-up through the selected sample geometries and  
78 boundary conditions. This section will be completed by a presentation of the  
79 gammadensimetry technique and its specific application in water profile measurements  
80 during wetting or drying phases.

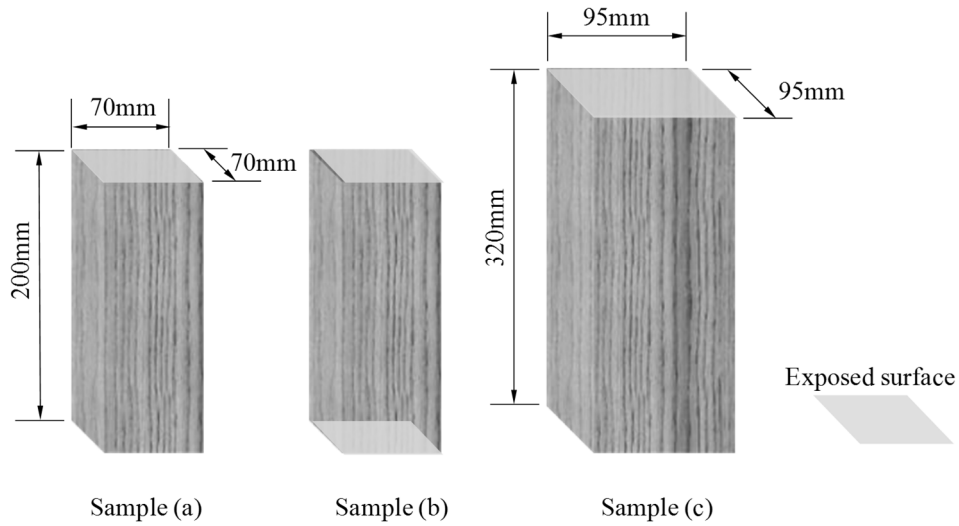
81 The numerical model and the determination of the diffusion parameters will be discussed  
82 in a second section. A nonlinear Fick's law will be coupled with an inverse method based  
83 on the downhill simplex method, which in turn allows optimizing the diffusion  
84 parameters in accordance with average moisture content measurements and water profiles  
85 determined by gammadensimetry method.

86 The last section will focus on experimental results. The method robustness will be  
87 validated by exhibiting the effects of boundary conditions and geometric dimensions.

## 88 **2 – Materials and methods: experimental set-up and numerical model**

### 89 **2.1 Materials and hydric loading**

90 The primary target of the experimental tests was to monitor moisture content evolution  
91 vs. time through various boundary conditions and geometries, using large samples at high  
92 relative humidity increments. As shown in Fig 1, three configurations were proposed  
93 considering moisture diffusion along the longitudinal direction. More precisely, the  
94 samples had been cut out along the anisotropic directions (i.e. Longitudinal L along the  
95 tree stem, Radial R perpendicular to the rings, and Tangential T parallel to the rings), with  
96 moisture diffusing along the longitudinal direction.



0.6	5.1	9.5	Initial moisture content (%)
97	97	86	Relative Humidity (%RH)

**Fig. 1** Moisture boundary conditions and sample geometries for the three cases

Under these conditions, only one or two faces were exposed to the external environment. Other faces were covered by two Parafilm layers to ensure unidirectional gas exchanges along the grain direction. Two geometries for the wood specimen, machined in Douglas fir (*Pseudotsuga menziesii* (Mirb.) Franco), were considered. For samples (a) and (b), their height equaled 200 mm (longitudinal direction) with a 70 mm x 70 mm cross-section (radial and tangential directions). In reality, specimens (a) and (b) were one in the same and had been repeatedly dried between the two experiments. This option allowed us to focus on the effect of boundary conditions. Sample (c) was the largest with a 320-mm height and a 95 mm x 95 mm cross-section, for the purpose of specially exploring ultimate scale and moisture loading effects.

110 For one thing, all specimens were conditioned in a dry environment using several  
 111 equilibrium moisture contents for  $w$ : less than 1% for sample (a), around 5% for sample  
 112 (b), and 9% for sample (c). The moisture content  $w$  is typically defined as the ratio of the  
 113 water mass  $M_{H_2O}$  to the dried or solid mass of wood  $M_s$ . Under a constant temperature  
 114 of approx. 19°C (+/-1°C), samples were placed in desiccators over saturated salt  
 115 solutions, which served to impose a constant relative humidity of around 97% RH for  
 116 samples (a) and (b), and roughly 86% RH for sample (c). Average moisture content is  
 117 basically determined by measuring weight during the sorption test.

## 118 **2.2 - Gammadensimetry method**

119 Gammadensimetry is a non-destructive method used to determine the density or moisture  
 120 content of civil engineering materials (Da Rocha *et al.*, 2001; Villain and Thierry, 2006;  
 121 Ferraz and Aguiar, 1985). This technique is based on the absorption of gamma rays  
 122 emitted by a radioactive source (in our case Cesium Cs<sup>137</sup>) and follows Lambert's law. To  
 123 determine moisture content at various heights, it is assumed that the wood material is  
 124 composed of three phases, namely solid  $s$  (dried wood), water  $w$  (bound water) and air  $a$ ,  
 125 such that:

$$126 \quad \ln\left(\frac{N_o}{N}\right) = \mu_s \cdot \rho_s \cdot x_s + \mu_w \cdot \rho_w \cdot x_w + \mu_a \cdot \rho_a \cdot x_a \quad (1)$$

127 where  $N_o$  is the number of incidental photons in the air,  $N$  the number of photons  
 128 crossing the sample of thickness  $X$  (m), and  $\mu_i$ ,  $\rho_i$  and  $x_i$  the mass absorption  
 129 coefficients (m<sup>2</sup>/kg), densities (kg/m<sup>3</sup>) and thicknesses (m) of phases  $i$  ( $i \in \{s, w, a\}$ ),  
 130 respectively. Let's remark that the air phase density and its mass absorption coefficient

131 can both be neglected. If the gamma ray crosses a thickness  $X$ , the following can be  
 132 expressed:

$$133 \quad X = \sum_i x_i \quad (2)$$

134 The moisture content  $w(t)$  is typically defined such that:

$$135 \quad w = \frac{M_{H_2O}}{M_s} = \frac{\rho_w \cdot x_w}{\rho_s \cdot x_s} \quad (3)$$

136 According to expression (1), thicknesses  $x_s$  and  $x_w$  at experimental time  $t$  are written as  
 137 follows:

$$138 \quad x_w(t) = \frac{(\ln \frac{N_0}{N})_t - (\ln \frac{N_0}{N})_{t=0}}{\mu_w \rho_w} + x_w(t=0) \quad (4)$$

$$139 \quad x_s(t) = x_s(t=0) = \frac{(\ln \frac{N_0}{N})_{t=0}}{\mu_s \rho_s + \mu_e \rho_s w_{(t=0)}} \quad (5)$$

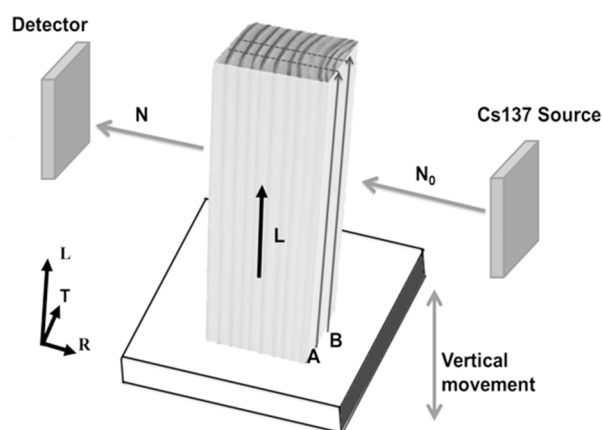
140 Due to swelling of the wood material under a sorption process, the water content may be  
 141 underestimated given that the thickness  $x_s$  at time  $t$  may be overestimated in the relation  
 142 (3). Nevertheless, the error on the moisture content due to the swelling effects in the  
 143 transverse plane (RT) is in the same magnitude order that the estimated swelling strains.  
 144 So, it can be neglected in regards to the dispersion of the measurements in link with the  
 145 further discussion about the possible uncertainties. In relation (5) therefore, it may be  
 146 assumed that thickness  $x_s$  crossed by the gamma ray does not vary during the sorption  
 147 process to simplify the determination of the moisture content.  
 148 Moreover, the moisture content profile was assumed to be homogeneous in the sample at  
 149 time  $t = 0$ . The calculus applied also had to integrate the Parafilm thickness in accordance  
 150 with expression (5).

151 For the various phases, the densities were:  $\rho_w = 1,000 \text{ kg/m}^3$  and  $\rho_s = 1,520 \text{ kg/m}^3$ . The  
152 mass absorption coefficient of each phase was calculated from its corresponding chemical  
153 analysis, while the elementary mass absorption coefficients for the radiation energy of  
154  $\text{Cs}^{137}$  are given, for instance, in the tables published by the U.S. National Bureau of  
155 Standards. For the water phase, the mass absorption coefficient was:  $\mu_w = 8.57 \cdot 10^{-3} \text{ m}^2/\text{kg}$ .  
156 As for the dried wood (solid) phase, it was assumed that wood is composed of cellulose,  
157 hemicellulose and lignin, thus leading to a mass absorption coefficient  $\mu_s = 8.17 \cdot 10^{-3}$   
158  $\text{m}^2/\text{kg}$ . More precisely, it was considered that the dried wood phase contained 50%  
159 carbon, 6% hydrogen and 44% oxygen in mass terms. Slight variations in these  
160 percentages however do exert a small impact on the final mass absorption coefficient  
161 value.

162 As shown in Fig 2, the moisture content profiles required placing the specimen in a plate  
163 that was vertically moved by a robot through the gamma ray beam at a 5-mm step.  
164 According to diffusion kinetics, it was assumed that moisture content is homogeneous  
165 along the radial direction for each cross-section and solely dependent on the longitudinal  
166 position of the gamma ray. Under these conditions, for each gamma ray position, the  
167 average moisture content in the cross-section was measured. Regular profile  
168 measurements were conducted throughout the experimental period (2 to 10 months).  
169 Several profiles were measured (2 for samples (a) and (b), 3 for sample (c)), yet only the  
170 averaged profile will be considered for the purpose of identifying diffusion parameters.

171 The viability of the gamma-ray method has been shown by Ferraz and Aguiar (Ferraz and  
172 Aguiar, 1985) for determining density and moisture content of wood samples. Relative  
173 deviations (absolute errors) between the traditional gravimetric method and the gamma-  
174 ray method have been estimated. The differences between the two methods are estimated  
175 up to 3% for samples with moisture content MC between 9 % and 30 % (relative error

176 inferior to 20%). The exactness of the gamma-ray method is limited mainly by errors  
 177 made in the determinations of  $N$  and  $N_0$  as a consequence of random disintegration; the  
 178 errors made in the determination in the other parameters (eg.  $x_s$ ) are negligible. Moreover,  
 179 in the case of the use of the Cesium  $Cs^{137}$  radioactive source, the sensitivity of the method  
 180 may be low because of the small differences between the mass absorption coefficients of  
 181 water and dried wood (solid) phase. But despite these possible absolute errors, it is  
 182 possible to obtain an average moisture content profile for large samples subjected to  
 183 hydric loading.



184  
 185 **Fig 2** Gammadensimetry profiles A and B for samples (a) and (b) along the longitudinal  
 186 direction (for sample (c), three profiles A, B and C have been considered)  
 187

188 Ultimately, the average moisture content profiles provided by gammadensimetry and  
 189 weighing must allow for the characterization of diffusion properties. The next sections  
 190 will propose an inverse method technique based on a mass transfer algorithm, along with  
 191 a downhill simplex method that serves to minimize the difference between numerical  
 192 model output and experimental measurements. This work will be limited to a uniaxial  
 193 approach due to moisture content homogeneity within the cross-sections.

### 194 **2.3 - Diffusion model**

195 Many models are proposed or developed to describe diffusion in wood: Fickian models,  
196 multi or not Fickian models, which can take into account dependence of diffusion  
197 coefficient on moisture content and take into account the surface exchanges. In the  
198 general case, the choice of the mass transport model deals with the necessity (or not) of  
199 separation of bound liquid, free water and vapor (Krabbenhof 2003; Perre and Turner,  
200 2008). In the present work, we are not in drying case from high water content where  
201 liquid, bound water and vapor cohabit, but below the saturation fibers point: in the  
202 hygroscopic domain, only bound water and vapor have to be considered. In this case,  
203 there is a common model with only one variable for both forms of water (Jakiela et al.,  
204 2008; Rozas et al., 2009; Olek et al., 2011; Da Silva et al., 2011) or model with separated  
205 variables (Frandsen et al., 2007, Krabbenhof 2003, 2004). . Then, differences between  
206 models can come from the choices for the treatment of the convective boundary  
207 conditions: relaxation term (Olek et al., 2016), hydrous surface exchange coefficient. It  
208 can be noticed that there is no consensus on the diffusion models which may have to be  
209 used and on the convective boundary conditions. Our assumptions and geometries allow  
210 us to use the common model which is described below.

211 The mass transfer process over time  $t$  is typically modeled using Fick's second nonlinear  
212 law. Fick's coefficients and the surface emission and diffusion coefficients are all  
213 described as phenomenological parameters since they can only be grasped or  
214 conceptualized through experience. According to isothermal conditions, the mass transfer  
215 process integrates a relationship focused on non-linearity between moisture content level  
216 and orthotropic diffusion tensor. From the perspective of a uniaxial representation  
217 characterized by the  $x$  coordinate, the time/space differential equation can be written as  
218 follows (Perre and Degiovanni, 1990; Merakeb *et al.*, 2006):

219 
$$\frac{\partial w}{\partial t} = \frac{\partial}{\partial x} \left( D_w(w) \cdot \frac{\partial w}{\partial x} \right) \quad (6)$$

220 The mass transfer process is principally driven by the diffusion property  $D_w$ . In wood  
 221 materials, this property is admitted to be nonlinear with respect to moisture content, in  
 222 accordance with the following form (Droin Josserand *et al.*, 1989):

223 
$$D_w(w) = D_o \cdot \exp(k \cdot w) \quad (7)$$

224 where  $D_o$  is the anhydrous moisture diffusion coefficient, and  $k$  a constant reflecting  
 225 the nonlinear effect.

226 According to boundary conditions, solving Fick's equation requires knowledge of the  
 227 surface moisture content, denoted  $w_\Omega$ . So, if  $S$  designates the hydrous surface exchange  
 228 coefficient, then the diffusion equation can integrate the following boundary limits:

229 
$$D_w(w) \frac{\partial w}{\partial x} = S \cdot (w_e(t) - w_\Omega(t)) \quad (8)$$

230 where  $w_\Omega$  is the surface moisture content. To take into account the exchanges between  
 231 water vapor molecules in air and bound water molecules in wood, it is commonly  
 232 considered to employ a virtual exchange layer defined by an instantaneous equilibrium  
 233 between external fibers and water vapor in the neighboring climatic environment. This  
 234 equilibrium is usually driven by sorption hysteresis and defined by the virtual moisture  
 235 content value, called  $w_e$  (Lasserre, 2000; Merakeb *et al.*, 2009).

236 Moreover, our problem can be reduced to characterizing  $D_o$ ,  $k$ ,  $S$  and  $w_e$ . The mass  
 237 transfer subroutine is implemented as part of the finite element method. However, the  
 238 problem is further reduced to a uniaxial configuration, and expressions (6) through (8)  
 239 are solved using a finite difference method based on a time discretization based on an  
 240 explicit Euler scheme (Zhou *et al.*, 2011; Liu and Simpson, 1999).

## 241 **2.4 - Downhill simplex method**

242 The downhill simplex method is introduced here to characterize diffusion properties  
243 (Nedler, 1965). This method consists of minimizing the objective function in using only  
244 function values and without calculating the derivative, so as to represent the gap between  
245 the moisture content evolution during experimental time and model results from the  
246 standpoint of least squares by means of adjusting diffusion parameters, such as diffusion  
247 coefficient  $D_o$ , nonlinear parameter  $k$ , hydrous surface exchange  $S$  and equilibrium  
248 moisture content  $w_e$ . For these four unknowns, the method considers a geometric  
249 polyhedron, called simplex, composed of 5 nodes, with each node representing a unique  
250 solution. Based on a hierarchy of errors for each solution, this algorithm reduces the  
251 geometric surface until convergence is reached. The vertices of this polyhedron will  
252 undergo geometric transformations in moving towards a global minimum (Lagarias *et al.*,  
253 1998). The simplex algorithm iterations correspond to simple algebraic operations on the  
254 polygon vertices for elementary geometric transformations (reflection, contraction and  
255 expansion) (Kelley, 1999). Each iteration transformation solely depends on a series of  
256 comparisons between objective function values corresponding to the calculated points  
257 and values of the polygon vertices to replace the worst vertex (maximum) by the new  
258 fixed point. The polygon is thus reflected, extended and reduced depending on the  
259 function shape until its optimum corresponds to a complete reduction of the simplex  
260 yielding the optimal solution. As demonstrated by Kouchade (2004), this method is well  
261 adapted to incomplete experimental curves.

262 The mass transfer process however performs two competing effects, in accordance with  
263 expressions (6) and (8). Based solely on the average moisture content evolution, the  
264 downhill simplex method does not distinguish the surface effect characterized by  $S$  and  
265  $w_e$  from the mass diffusion characterized by  $D_o$  and  $k$ . When limited to the average

266 moisture content data, the minimization method can actually yield an infinite number of  
267 solutions. The use of water profiles provided by gammadensimetry could ensure an  
268 acceptable level of separation between surface and mass effects.

### 269 **3 - Results and discussion: moisture content profiles of sorption tests and** 270 **identifications of diffusion parameters**

271 This section proposes comparing the two methods for identifying diffusion parameters by  
272 taking into account both moisture loading and sample geometry. This methodology will  
273 be applied to samples (a) and (b) and then to sample (c). The diffusion parameters will be  
274 discussed afterwards.

#### 275 **3.1 - Identification of diffusion parameters for sample (a): reference case**

276 Sample (a) is characterized by just one surface of moisture content exchange, with initial  
277 drying in an oven at 103°C. As shown in Fig. 3 after 81 days of adsorption, the average  
278 moisture content increased to only 14%, i.e. far below the equilibrium moisture content  
279 estimated to lie around 22% at about 20°C, according to Loulou (2013) and Merakeb *et*  
280 *al.* (2009). The equilibrium moisture content value is highly sensitive to both the moisture  
281 and thermal loading; hence, the level of precision is approx. +/-2%, especially for a high  
282 Relative Humidity loading.

283 Diffusion parameters are normally characterized using a simple weighing of small  
284 samples corresponding to average moisture content information over time; this procedure  
285 is referred to as standard identification. For this standard identification, the equilibrium  
286 state is normally raised, leading to a possible identification of the diffusion parameters.  
287 In our particular case, let's set the equilibrium moisture content value  $w_e$  as unknown. In  
288 our example therefore, this approach is being compared on five weighing measurements  
289 (at 3, 10, 18, 25 and 81 days) with a so-called coupled identification using crossing

290 weights and gamma-ray measurements.

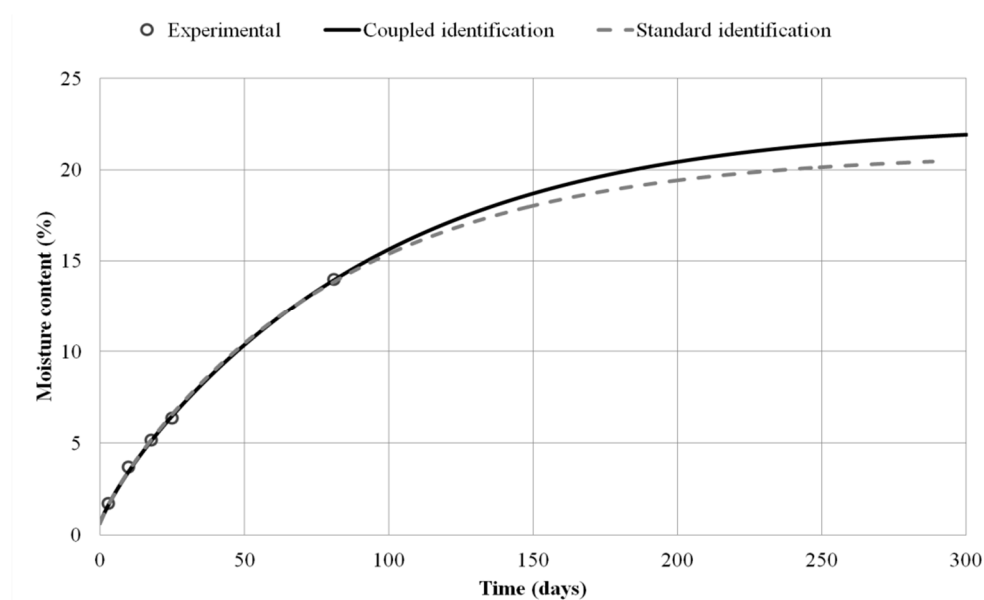
291 The comparison between these two identification methods is presented in Fig. 3 and Fig.  
292 4, in accordance with identified diffusion parameters (see Table 1). The nonzero values  
293 obtained for the non-linearity coefficient and the rather low hydrous surface exchange  
294 coefficient serve to validate the hypotheses of nonlinear diffusion and exchanges by  
295 hydrous convection.

296 **Tab 1** Diffusion parameters for sample (a)

Identification method	$D_0 (m^2 \cdot s^{-1})$	$k$	$S (m \cdot s^{-1})$	$w_e$
Standard identification	$4.50 \cdot 10^{-9}$	1.12	$5.03 \cdot 10^{-8}$	20,6%
Coupled identification	$3.27 \cdot 10^{-9}$	1.94	$4.73 \cdot 10^{-8}$	22,5%

297

298 Results highlight the sensitivity of identification by means of the inverse method. Fig. 3  
299 illustrates that in terms of average moisture content evolution, various diffusion  
300 parameters can yield the same results, especially within the experimental time frame.



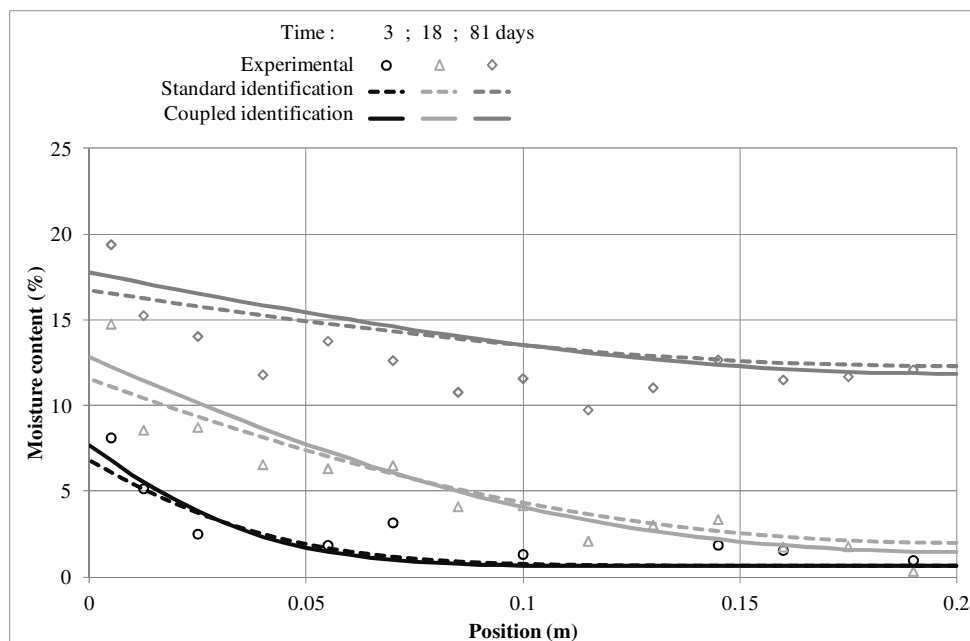
301

302 **Fig. 3** Results of standard and coupled identification in terms of

303 average moisture content evolution for sample (a)

304

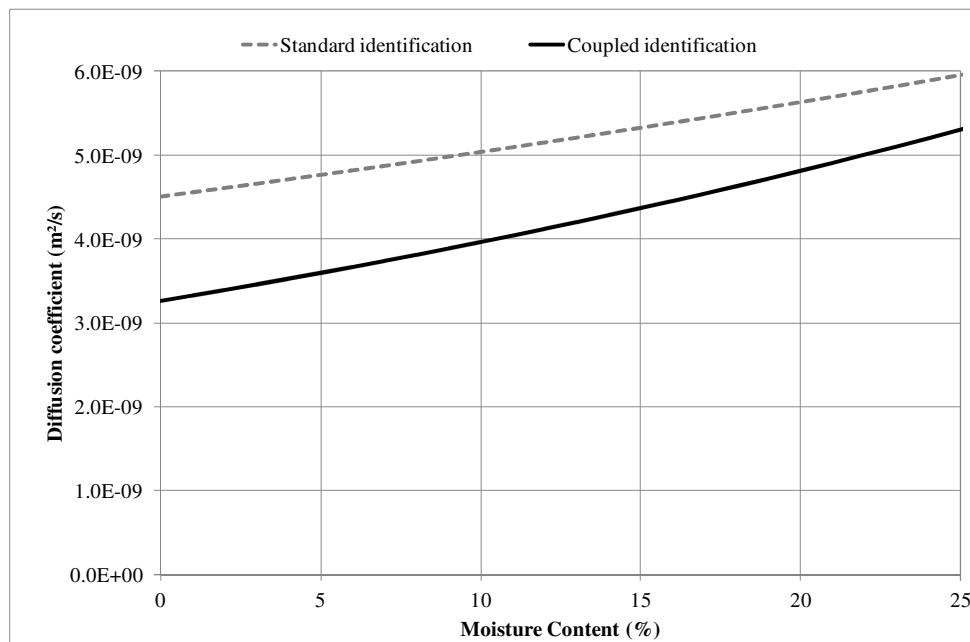
305 The coupled identification was performed using five profiles (at each weighing time), but  
 306 only three profiles have been presented for the sake of clarity. The profile results  
 307 displayed in Fig. 4 however reveal slight differences. As explained previously, it can be  
 308 observed that the gammadensimetry measurements present dispersions around an average  
 309 profile value. Despite this dispersion (and some anomalous points), it is still possible to  
 310 compare the experimental and numerical profiles. Experimentally, we can observe that  
 311 the moisture content first increases on the exposed face and only in the first quarter of the  
 312 sample (day 3), then the moisture gradient decreases while the moisture content increases  
 313 up to the whole sample and the sealed face (day 81). Numerically, the main difference  
 314 between the profiles from the standard identification (that does not take into account the  
 315 experimental profiles) with those from the coupled identification concerns the higher  
 316 moisture content values on the exposed face as seen experimentally.



317

318 **Fig. 4** Results of standard and coupled identification, in terms of moisture content  
 319 profiles for sample (a)

320 As regards the identified diffusion parameters, let's note a slight difference in exchange  
 321 surface coefficient of around 6% and a difference in the anticipated value of  $w_e$  (9%).  
 322 The main differences actually pertain to the diffusion parameter characterization and its  
 323 property of non-linearity. According to expression (7), the identification method produces  
 324 a great difference (of up to 25%) in the diffusion parameter evolution vs. moisture content  
 325 (Fig. 5).



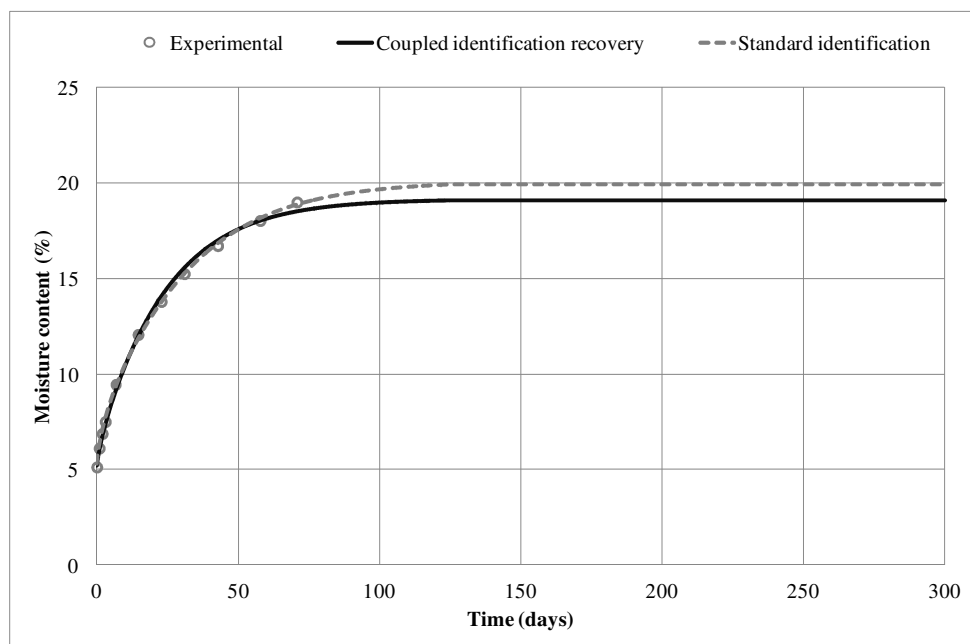
326

327 **Fig. 5** Diffusion coefficient vs. moisture content within the hygroscopic domain  
 328 given by the two identifications performed on the results of sample (a)

329 According to a homogeneity assumption on the sample however, parameters  $D_o$  and  $k$   
 330 should be intrinsic material properties, while the surface exchange coefficient is  
 331 somewhat intrinsic to the experiment and its exposure conditions. The small correction  
 332 due to the coupled identification on its value has a significant effect on the diffusion  
 333 parameters values and we can expect a better identification of this lasts.

334 **3.2 - Diffusion parameters identification for sample (b): effect of boundary**  
335 **conditions**

336 In the following discussion, both boundary and initial conditions will be the focus of an  
337 investigation considering two surface exchanges and various initial moisture contents.  
338 According to Figure 1, this second experiment will concentrate on sample (b). To  
339 investigate the decoupling between the intrinsic diffusion coefficient ( $D_0$  and  $k$ ) and the  
340 surface exchange coefficient  $S$ , sample (b) is to be the same specimen as sample (a), yet  
341 the initial conditions and exchange conditions have been modified. After the first  
342 experiment, the sample is once again dried until a homogeneous moisture content of 5%  
343 is obtained and two faces are in contact with the environment. As shown in Fig. 6 after  
344 less than 80 days of adsorption, the average moisture content has already risen to 19%,  
345 i.e. not far below the expected equilibrium moisture content.



346  
347 **Fig. 6** Results from both the standard and coupled (recovery from sample (a))  
348 identification, in terms of average moisture content evolution for sample (b)

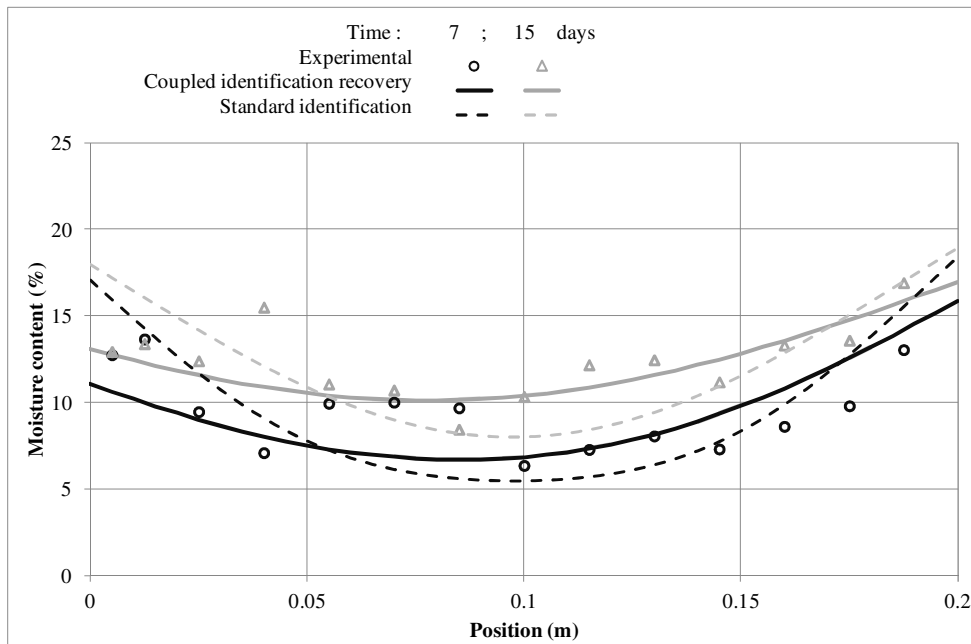
349 These same approaches are then proposed in using diffusion coefficients from the coupled  
350 identification of sample (a) in order to calibrate equilibrium moisture content and a

351 second surface exchange coefficient  $S'$  that characterizes the additional surface  
 352 (assumption of a moisture content exchange asymmetry: surfaces and exposition being  
 353 the same, we can nevertheless not be sure that surface states, with wood rings, are so). It  
 354 can be noticed that the asymmetry may be not measured by the gamma-ray method owing  
 355 to moisture content dispersion. According to the diffusion properties listed in Table 2, the  
 356 average moisture content evolution and moisture content profiles can now be plotted  
 357 (Figs. 6 and 7).

358 **Tab 2** Diffusion parameters for sample (b)

Identification method	$D_o \left( m^2 \cdot s^{-1} \right)$	$k$	$S \left( m \cdot s^{-1} \right)$	$S' \left( m \cdot s^{-1} \right)$	$w_e$
Standard identification	$1.24 \cdot 10^{-9}$	2.58	$1.43 \cdot 10^{-7}$	$2.72 \cdot 10^{-7}$	20.1%
Coupled identification (recovery from sample (a))	<b><math>3.27 \cdot 10^{-9}</math></b>	<b>1.94</b>	<b><math>4.73 \cdot 10^{-8}</math></b>	$1.86 \cdot 10^{-7}$	19.2%

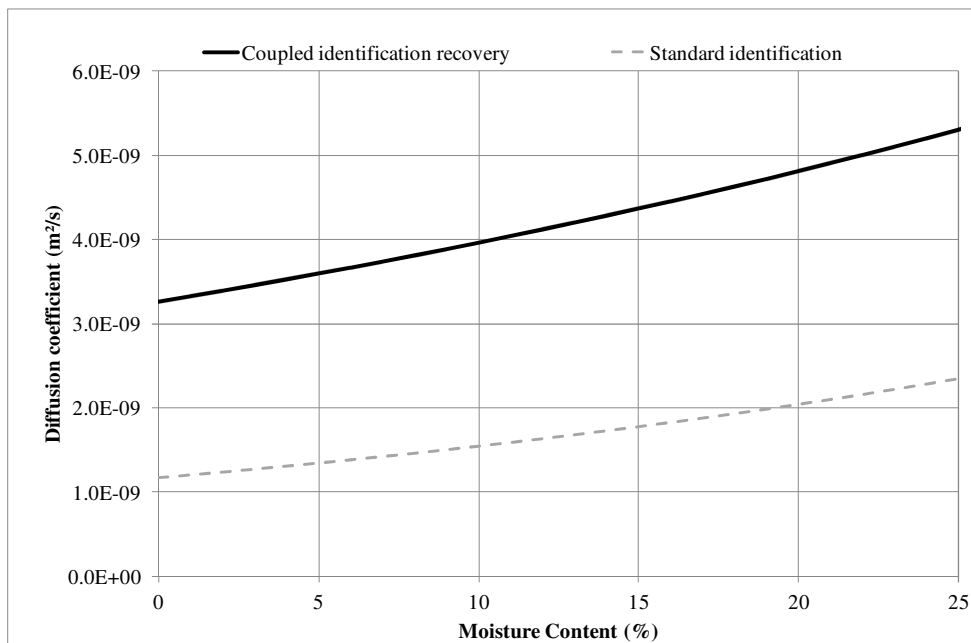
359  
 360 In optimizing  $S'$  we were able to find a relative good fit of the average moisture content  
 361 evolution obtained from a dozen weighing measurements and the only two moisture  
 362 profiles recorded at 7 and 15 days (with gamma measurements once again exhibiting  
 363 dispersions) with higher moisture content values recorded on the second face. The  
 364 coupled identification method leads to detecting clearer moisture exchange differences  
 365 between the two faces, as presented by the moisture profiles in Fig. 7. The standard  
 366 identification presents two main defaults, less in accordance with the experimental  
 367 profiles: it quickly leads to high moisture content to both faces and in opposite the  
 368 moisture content in the middle of the sample should remain low. At last, by considering  
 369 the only weighing, it cannot easily estimate separated values for the two surface exchange  
 370 coefficients.



371

372 **Fig. 7** Results from standard and coupled (recovery from sample (a)) identification,  
 373 in terms of moisture content profiles for sample (b)

374 The two profiles seem to be sufficient for determining the nonlinear characteristic of the  
 375 diffusion process, as observed by comparing diffusion coefficient variations vs. the  
 376 moisture content (Fig. 8) derived by both the standard and coupled identifications.



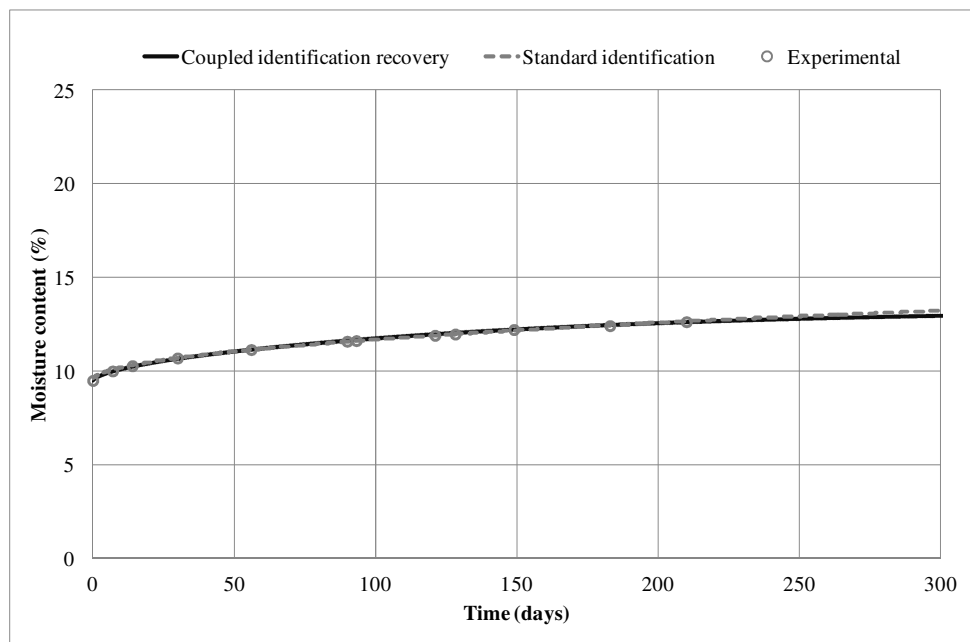
377

378 **Fig. 8** Diffusion coefficient vs. moisture content within the hygroscopic domain,  
 379 as provided by the identification methods performed on the results of sample (b)

380 As a matter of fact, this second experiment confirms the differences between coupled and  
381 standard identification techniques, with the latter most likely yielding less intrinsic  
382 results. In this case, the numerical profile with the coupled method allows for a better  
383 agreement with the experimental profile.

### 384 3.3 - Diffusion parameters identification for sample (c): scale effect

385 This experiment on sample (c) is based on the same single-face exposure adopted for  
386 sample (a). As specified in Figure 1, the dimensions and moisture conditions of sample  
387 (c) are different in that sample (c) has been previously conditioned in a dry chamber  
388 corresponding to the equilibrium moisture content around 9.5%. In terms of average  
389 moisture, the evolution of this sample is plotted in Fig. 9.



390

391 **Fig. 9** Results of the coupled identification method with recovery from sample (a) and  
392 standard identification, in terms of average moisture content evolution for sample (c)

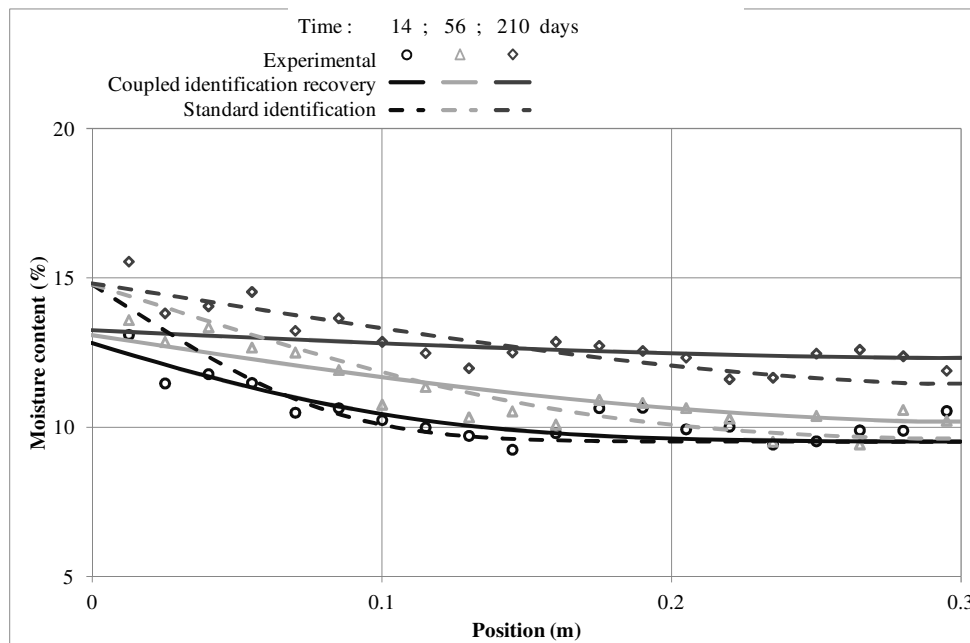
393 The experimental test was stopped after 220 days and a dozen weighing measurements,  
394 with the average water content equaling about 13%. At equilibrium, the moisture content  
395 might have been about 15% according to Loulou (2013). The three profiles measured at

396 14, 56 and 210 days are plotted in Fig. 10. The results of the standard and coupled  
 397 identification methods are summarized in Tab 3.

398 **Tab 3** Diffusion parameters for sample (c)

Identification method	$D_o \left( m^2 \cdot s^{-1} \right)$	$k$	$S \left( m \cdot s^{-1} \right)$	$w_e$
Standard identification	$9.33 \cdot 10^{-10}$	4.64	$2.64 \cdot 10^{-6}$	14.8%
Coupled identification (recovery from sample (a))	<b><math>3.27 \cdot 10^{-9}</math></b>	<b>1.94</b>	$2.35 \cdot 10^{-7}$	13.3%

399

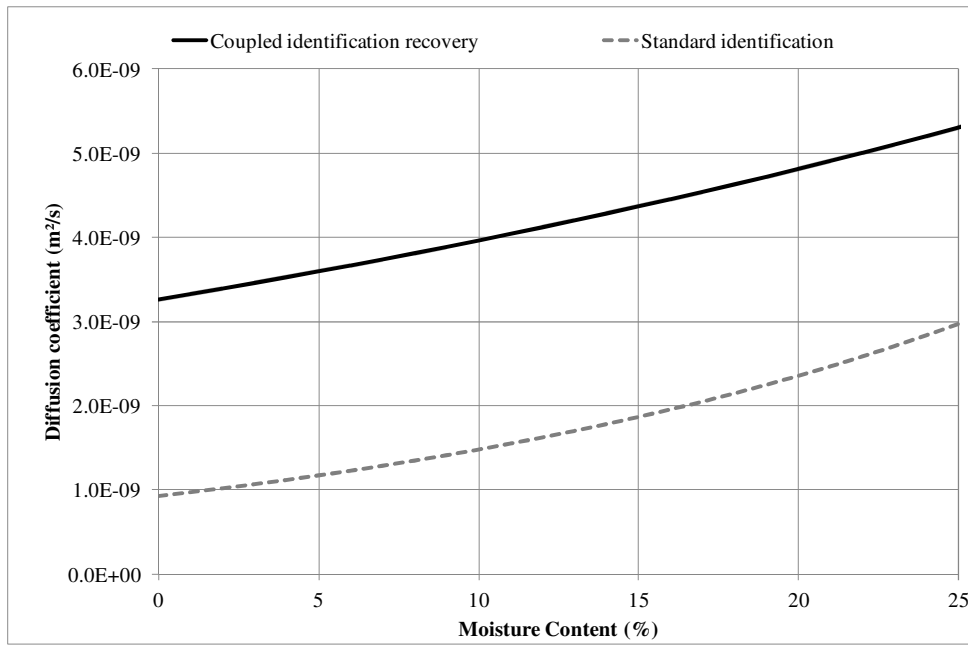


400

401 **Fig. 10** Results from the standard and coupled (with recovery from sample (a))  
 402 identification, in terms of moisture content profiles for sample (c)

403 Lastly, this third experiment again confirms the differences between coupled and standard  
 404 identification as the numerical profiles with the coupled method allows, in this last case,  
 405 for a better correlation with the experimental profiles: the moisture content evolution  
 406 estimated on the exposed face is better predicted in the first moments (days 14 and 56),  
 407 as the moisture content distribution in the main part (from position 0.1 to 0.3m) of the  
 408 sample (until day 210). We can just note that the equilibrium moisture content seems to  
 409 be a little weak regarding to the value recorded near the exposed face, this time better

410 represented by standard identification's last profile (days 210). More specifically, the two  
411 methods differ in terms of hydrous convection kinetics near the exchange surface.  
412 Significant differences are also observed in terms of diffusion coefficient evolution as a  
413 function of water content (Fig. 11).



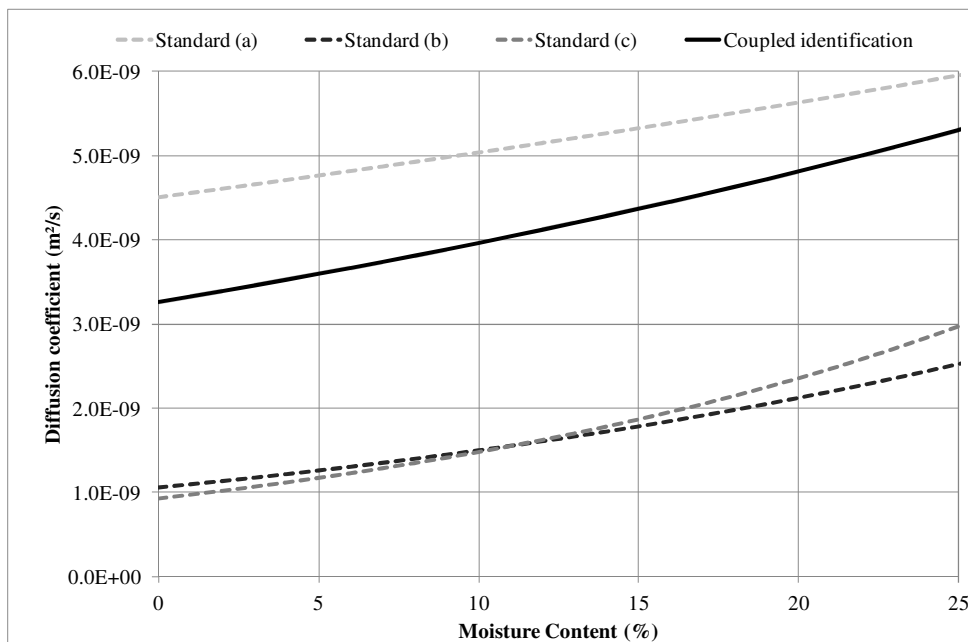
414

415 **Fig. 11** Diffusion coefficient vs. moisture content within the hygroscopic domain,  
416 as output by the two identification methods performed on the results of sample (c)

### 417 3.4 - Discussion

418 The difference between these two identification methods (standard and coupled), as  
419 compared for sample (a), may be explained in a series of remarks. First of all, because  
420 the standard identification is based on a global, or averaged, experimental moisture  
421 content monitoring, the number of diffusion parameters is capable of inducing self-  
422 optimization, in correlation with one measurement point per time interval. In this case,  
423 the surface exchange coefficient  $S$  can correct an error when characterizing the diffusion  
424 coefficient determination; moreover, as shown in Fig. 3, various identified parameters  
425 may be consistent with the time - average moisture content curve. Hence, the standard  
426 identifications for samples (a), (b) and (c) show significant differences on diffusion

427 coefficients (Fig. 12). The moisture content profiles given by gammadensimetry method  
 428 make it possible to correct the specimen diffusion parameters along the moisture content  
 429 gradient. All experimental time points represent a numerical constraint for the inverse  
 430 method algorithm, thus facilitating the optimization of diffusion parameters. The unique  
 431 couple of diffusion coefficients identified in the reference case (i.e. sample (a)), along  
 432 with the proposed coupled method, is able to reproduce both average moisture content  
 433 evolution and profiles for the two other study cases with different boundary conditions  
 434 and geometric dimensions (samples (b) and (c)).



435

436 **Fig. 12** Diffusion coefficient vs. moisture content within the hygroscopic domain,  
 437 as provided by the two identification methods performed on the results of samples (a),  
 438 (b) and (c)

439 Our proposed experimental method deals with robustness of identification of diffusion  
 440 parameters, usually made with only weighing: with a spatial measurement of water  
 441 content distribution we fill in a lack of information that could fault any sophisticated  
 442 model. Indeed, this study has exposed the remediable flaws of the standard identification  
 443 method, the weighing appearing insufficient with sparsely measurement points far from

444 equilibrium. Although characterization does allow for an acceptable modeling of the  
445 average moisture content evolution, it is not always possible to easily reproduce the  
446 profiles within the material. The balance between the hydrous exchange by convection  
447 and diffusion in the material can lead to a significant number of satisfactory datasets for  
448 the average moisture content. Moreover, should the experimental time frame prevent  
449 achieving moisture equilibrium, the diffusion kinetics errors can lead to an incorrect  
450 extrapolation of equilibrium moisture and induce errors in the estimation of sorption  
451 isotherms. In this case, a better characterization of diffusion properties, and more  
452 specifically convective parameters, at the beginning of the test can increase diffusion  
453 extrapolation accuracy. The moisture content profiles do yield better information for a  
454 better fit of the time moisture content evolution.

455 Although these profiles contain a high level of experimental noise, the coupled  
456 characterization method does enable constraining the minimization algorithm in order to  
457 limit the number of possible combinations, in terms of diffusion properties, by  
458 highlighting the moisture effects due to convective processes. Such a feature makes this  
459 method more accurate and robust with sets of parameters intrinsic to the studied material,  
460 thus offering, via the use of a diffusion model, a more realistic prognosis beyond  
461 experimental observations. At last, it may be useful for applications in the field of in-situ  
462 monitoring of structural timber elements and it will certainly be improved in the future  
463 thanks to more elaborated models.

#### 464 **4 - Conclusion and outlook**

465 This work has proposed an experimental protocol for characterizing nonlinear diffusion  
466 properties. The coupling between a simple weighing of samples, corresponding to an  
467 average moisture variation identification, with a gammadensimetry technique has been

468 presented. Such a coupling allows for a realistic separation between diffusion kinetics  
469 through the cross-section and the moisture content surface exchange. Moreover, the  
470 nonlinear diffusion coefficient is better determined by taking into account the moisture  
471 content profiles given by the gamma-ray method. Scale effects, as well as the studied  
472 boundary and initial conditions, enable concluding the robustness of this approach in  
473 measuring some really intrinsic properties.

474 Moisture profiles have provided us with certain information during the start of adsorption;  
475 they allow for a better identification of the initial diffusion times in the vicinity of  
476 boundary elements. This additional information increases the model's potential to predict  
477 moisture content evolution vs. time. We are now able to propose other experimental  
478 protocols for characterizing diffusion without finding moisture equilibrium. In this  
479 specific case, this algorithm may be used to determine diffusion properties during  
480 moisture buffer tests in which outdoor humidity conditions are in a harmonic solicitation  
481 pattern.

482 Regarding the monitoring of timber structures, the diffusion behavior of elements must  
483 be known in order to predict long-term mechanical responses and durability of the  
484 structures. The gammadensimetry technique offers certain information about the moisture  
485 content gradient state; however, this method cannot be generalized to outdoor monitoring.  
486 A perspective on this work is the development of a non-destructive method to allow  
487 measuring moisture gradients in the cross-section. One solution consists of replacing the  
488 gammadensimetry method by a 2D or 3D resistive method coupled with a multiplexing  
489 technology and a numerical inversion method.

490 **References**

- 491 Baettig R., Rémond R., Perré P., Measuring moisture content profiles in a board during  
492 drying: a polychromatic x-ray system interfaced with a vacuum/pressure laboratory kiln,  
493 *Wood Science and Technology*, 40(4), 2006, pp. 261–274.
- 494 Colmars J., Dubois F., Gril J., One-dimensional discrete formulation of a hygrolock  
495 model for wood hygromechanics, *Mechanics of Time-Dependent Materials*, 18(1), 2014,  
496 pp. 309-328.
- 497 Da Rocha M.C., Da Silva L.M., Appoloni C.R., Portezan Filho O., Lopes, F., Melquiades,  
498 F.L., et al., Moisture profile measurements of concrete samples in vertical water flow by  
499 gamma ray transmission method., *Radiat Phys Chem*, 61 (3-6), 2001, pp.567-9.
- 500 Dubois F., Petit C., Sauvat N., Peuchot B., Diagnostic et comportement des ponts à  
501 ossature bois : Application au pont de Merle, *European Journal of Civil Engineering*, 10  
502 (2), 2006, pp. 191-208
- 503 Dubois F., Husson J.M., Sauvat N., Manfoumbi N., Modeling of the viscoelastic  
504 mechano-sorptive behavior in wood, *Mechanics of Time-Dependent Materials*, 16(4),  
505 2012, pp. 439-460.
- 506 Droin Jossierand A., Vergnaud J.M. Taverdet, J.L. Modeling the process of moisture  
507 absorption in three dimensions by wood samples of various shapes: cubic,  
508 parallelepipedic. *Wood Science and Technology*, 17. VIII., Vol 23, Issue 3, 1989, pp.259–  
509 271.
- 510 Ferraz E.S.B., Aguiar O., Gamma-ray attenuation technique for determining density and  
511 water content of wood samples, *IPEF*, 30, ago.1985, pp 9-12.
- 512 Frandsen H.L., Damkilde L., Svensson S., A revised multi-Fickian moisture transport  
513 model to describe non-Fickian effects in wood, *Holzforschung*, 61, 2007, pp. 563-572.

514 Jakiela S., Bratasz L., Kozlowski R., Numerical modeling of moisture movement and  
515 related stress field in lime wood subjected to changing climate conditions, *Wood Science*  
516 *and Technology*, 42(21), 2008, pp. 21-37.

517 Kelley C.T., *Iterative Methods for Optimization*, North Carolina State University.  
518 Raleigh, *Society for Industrial and Applied Mathematics*, 1999, pp. 135-141.

519 Kouchade A.C., Détermination en routine de la diffusivité massique dans le bois par  
520 méthode inverse à partir de la mesure électrique en régime transitoire, PhD Thesis,  
521 Engref, Nancy, 2004.

522 Krabbenhoft K., Moisture transport in wood: a study of physical-mathematical models  
523 and their numerical implementation. PhD Thesis, Department of Civil Engineering  
524 Technical University of Denmark, 2003.

525 Krabbenhoft K., Damkilde L., A model for non Fickian moisture transfer in wood,  
526 *Materials and Structures*, 37, 2004, pp. 615-622.

527 Lagarias J.C., Reeds J. A., Wright M. H., Wright P. E., Convergence Properties of the  
528 Nelder-Mead Simplex Method in Low Dimensions, *SIAM Journal*, 1998, pp. 112-147.

529 Lasserre B., Modélisation thermo-hygro-mécanique du comportement différé de poutres  
530 de structure en bois, PhD Thesis, University of Bordeaux I, 2000.

531 Liu J.Y., Simpson W.T., Inverse determination of diffusion coefficient for moisture  
532 diffusion in wood. *Proceedings of 33rd ASME National Heat Transfer Conference : Heat*  
533 *and mass transfer in porous media*, August 15-17, 1999, Albuquerque, New Mexico.

534 Loulou L., Durabilité de l'assemblage mixte bois-béton collé sous chargement hydrique,  
535 PhD Thesis, Université Paris Est, 2013.

536 Manfoumbi N., Adaptation réglementaire de l'Eurocode 5 aux essences tropicales dans  
537 un climat tropical, PhD Thesis, University of Limoges, 2012.

538 Manfoumbi N., N’Guyen T. A., Angellier N., Dubois F., Ulmet L., Sauvat N.,  
539 Experimental and numerical aspects in diffusion process characterization in tropical  
540 species, *European Journal of Environmental and Civil Engineering*, 18 (9), 2014, pp.  
541 963-982.

542 Merakeb S., Dubois F., Petit C., Sauvat N., Couplage hydromécanique dans le processus  
543 de diffusion dans le bois, *European Journal of Civil Engineering*, 10 (2), 2006, pp. 225-  
544 251.

545 Merakeb S., Dubois F., Petit C., Modeling of the sorption hysteresis for wood, *Wood*  
546 *Science and Technology*, 43 (7-8), 2009, pp. 575-589.

547 Nedler J.A., Downhill simplex method, *Computer Journal*, 7, 1965, pp. 308-313.

548 Olek W., Perre P., Weres J., Implementation of a relaxation equilibrium term in the  
549 convective boundary condition for a better representation of the transient bound water  
550 diffusion in wood, *Wood Science and Technology*, 45, 2011, pp. 677-691.

551 Olek W., Rémond R., Weres J., Perré P., Non-Fickian moisture diffusion in thermally  
552 modified beech wood analyzed by the inverse method, *International Journal of Thermal*  
553 *Sciences*, 109, 2016, pp. 291-298.

554 Da Silva W.P., Da Silva L.D., Silva E., C.D.M.P.S., Nascimento P.L., Optimization and  
555 simulation of drying processes using diffusion models : application to wood drying using  
556 forced air at low temperature, *Wood Science and Technology*, 45, 2011, pp.787-800.

557 Perre P., Degiovanni A., Simulation par volumes finis des transferts couplés en milieux  
558 poreux anisotrope : séchage du bois à basse et haute température, *International Journal*  
559 *of Heat and Mass Transferts*, 33(11), 1990, pp.2463–2478.

560 Perre P., Turner I.W., A mesoscopic drying model applied to the growth rings of  
561 softwood: mesh generation and simulation results, *Maderas. Ciencia y tecnologia*, 10(3),  
562 2008, pp. 251-274.

563 Rozas C., Tomaselli I., Zanoelo E. F., Internal mass transfer coefficient during drying of  
564 softwood (*Pinus elliottii* Engelm.) boards, *Wood Science and Technology*, 43 2009, pp.  
565 361-373.

566 Villain G and Thierry M.. Gammadensimetry: a method to determine drying and  
567 carbonation profiles in concrete, *ND&E Int.*, 39 (4), 2006, pp.328-337.

568 Zhou Q., Cai Y., Xu Y., Zhang X., Determination of moisture diffusion coefficient of  
569 larch board with finite difference method, *BioRes*, 6 (2), 2011, pp. 1196-1203.